

Developing Strategies for Characterization of Cellular Senescence

A Major Qualifying Project Report

Submitted to the faculty

Of the

Worcester Polytechnic Institute

In partial fulfillment of the requirements for the

Degree of Bachelor Science

In Biochemistry

By

Victoria Ruhl

Date: March 1st, 2007

Approved:

Professor Jill Rulfs, WPI Advisor
Dept. of Biology/Biotechnology

Dr. Paul Kaufman, PhD
Program in Gene Function and
Expression
University of Massachusetts
Medical School

Table of Contents

ABSTRACT	4
INTRODUCTION	5
Cellular Senescence	5
ARID4B (AT rich interactive domain 4B)	7
Prohibitin	8
ASF1a (anti-silencing function 1 a)	9
METHODS	10
Cell Culture	10
Immunofluorescence (IF)	10
Immunoblots	10
Transfection of 293T Cells to Generate Lentiviruses	11
Transfection of 293gag/pol Cells to Generate Retroviruses	11
Viral Titers of Lentiviruses and Retroviruses	12
Infection of Primary and Transformed Human Cells with Lentiviruses and Retroviruses	12
Protein Purification of the ARID4B domain and ARID4B exon 16	12
Glutathione Sepharose Column Purification	13
Q Sepharose Column Purification	14
CuCl ₂ Staining, Electroelution, and Lyophilization	14
RESULTS	15
ARID4B Domain and Exon 16 Antibody Purification and Production	15
Depletion of Prohibitin with Retroviral miRNA	21
Depletion of ASF1a with Lentiviral miRNA	22
DISCUSSION	23
ARID4B	23
Prohibitin	24

ASF1a	25
Conclusions	25
REFERENCES	27

Abstract

Cellular senescence is a tumor suppressive mechanism that limits growth of human cells by causing cell cycle arrest in G1 phase. Senescence has been of wide interest in recent years because of its link to human cancers. The onset of senescence is caused by repression of transcription through the remodeling of chromatin. This project is focused on developing strategies to identify the role of three chromatin regulating proteins implicated in senescence—ASF1a, ARID4B, and prohibitin.

Introduction

Cellular Senescence

Cellular senescence is a mechanism that limits growth of human cells in culture by causing cell cycle arrest in G1 phase. Two major causes of senescence have been identified. One cause is the accumulated telomere shortening that increases during each S phase in the absence of the enzyme, telomerase. This telomere shortening results in a DNA damage response (Ben-Porath, 2004).

A second type of senescence can occur prematurely in young adult cells and is caused by various stresses including activated oncogenes, oxidative stress, or DNA damage (Serrano, 1997). Regardless of the cause, retinoblastoma (Rb) and p53 are the major activators of senescence (Figure 1). Rb activates senescence by repressing the transcription of E2F activated target genes, which are required for cell cycle progression. The p16^{INK4a} and p53 proteins activate Rb through two separate pathways (Figure 1). The p53 protein promotes cell cycle exit by stimulating expression of p21, a cyclin-dependent kinase inhibitor (CKI) that activates Rb to block the cell cycle. The p16^{INK4a} protein activates Rb by inhibiting a different subset of cyclin-dependent kinases (Ben-Porath, 2004).

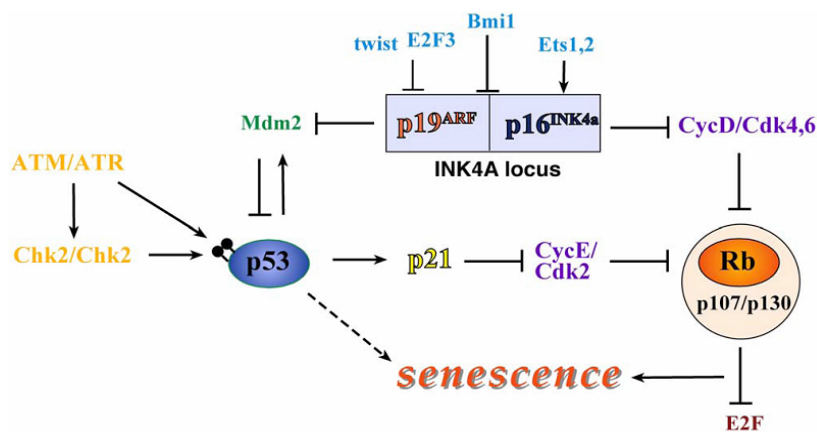


Figure 1: The pathways of senescence. Rb and p53 are the major activators of senescence. The activation of p21 by p53 causes Rb to activate and repress transcription of E2F target genes. p16^{INK4a} also activates Rb through a separate pathway. In human cells, p53 can activate senescence independently of Rb. ATM/ATR and Chk1/Chk2 proteins activate p53 through phosphorylation. (Pathway scheme from Ben-Porath, 2004)

Senescence is of wide interest because it acts as a tumor suppressive response. Study of tumor cells and senescence has shown that the p53 and Rb pathways that are important to establish senescence are mutated in most human cancers (Campisi, 2001) suggesting that inactivation of these pathways is a critical step in tumorigenesis. *In vivo* studies in mice and humans have revealed that premalignant tumors are composed mainly of senescent cells whereas fully malignant tumors are almost completely devoid of senescent cells, suggesting that senescence serves as a barrier to tumorigenesis (Braig, 2005; Chen, 2005; Collado, 2005). Therefore, drugs that can induce senescence are being further studied as cancer therapeutic agents.

There are markers that clearly define cells that have become senescent. This has been most heavily studied in human diploid fibroblasts. First, the cells change morphology. Upon senescence, fibroblasts become more flat and elongated than normal cells (Figure 2) and have higher senescence-associated β -galactosidase activity that can be histochemically detected at pH 6 (Dimri, 1995). Additionally, markers detected by immunofluorescence (IF) can be a key tool in determining if cells have become senescent. Senescence associated heterochromatin foci (SAHF) are condensed chromosomes that are seen in many types of senescent mammalian cells (Zhang, 2005). The correlation of chromosome condensation and cell cycle exit in these cells suggests that chromosomal remodeling proteins are involved in establishing and maintaining the senescent state of human fibroblasts. This project is focused on three sets of chromatin proteins implicated in senescence—ASF1a, ARID4B, and prohibitin.

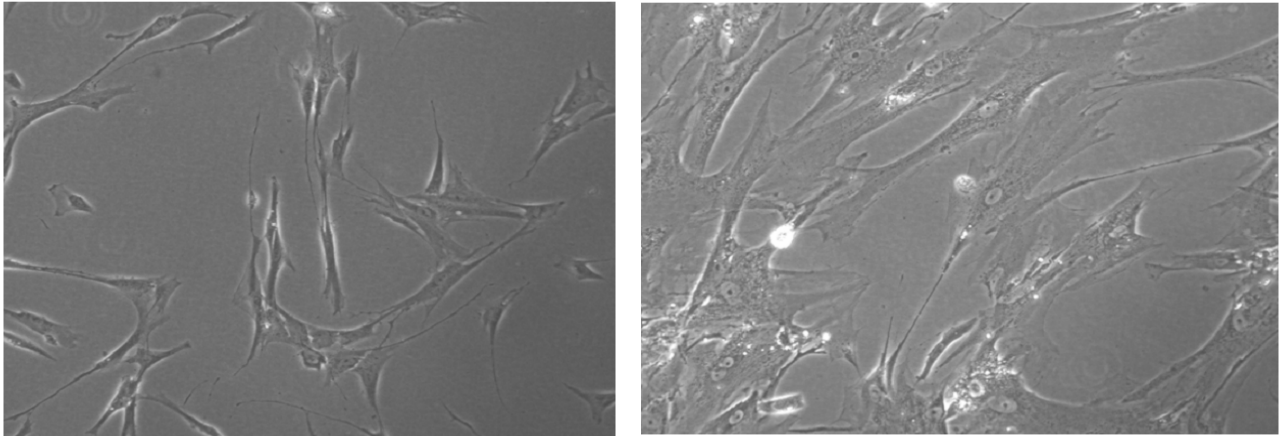


Figure 2: Morphology change in human diploid fibroblast IMR90 cells upon senescence. A photograph of IMR90 cells at population doubling 25 (left panel), shows growing cells with a normal morphology. A photograph of the same cells at population doubling 85 (right panel) shows senescent cells with a more flat and elongated morphology.

ARID4B (AT rich interactive domain 4B)

ARID4B is thought to be a key player in cellular growth control for several reasons. One study has shown that the overexpression of ARID4B in H1299 cells (a human lung cancer cell line) induced a senescence response (Binda, 2006). However, this has not yet been tested in human primary cell lines. ARID4B has also been named BRCAA1 (breast cancer associated antigen 1) because a truncated version of this protein was found to be present in 65% of tested breast cancer specimens, with 100% negativity in non-cancerous tissues (Cui, 2004). Together, these data suggest that ARID4B may be a growth regulatory protein that normally inhibits proliferation but can become oncogenic when mutated.

In addition to its relation to cancer, ARID4B is also involved in chromosome biology. ARID4B is a subunit of the Sin3a HDAC (histone deacetylase complex), which removes acetyl groups from histone termini. HDACs are associated with repressed chromatin structures such as SAHF (Narita, 2003). Consistent with a role in chromosome regulation, a tudor and a chromo domain have both been identified in the ARID4B protein (Figure 3).

Both of these domains bind methylated histones, which further shows that ARID4B could likely be a component in the remodeling of chromatin during the onset of senescence.

Preliminary studies in the Kaufman laboratory determined that the only commercially available α -ARID4B antibody does not specifically detect overexpression of ARID4B on an immunoblot. The study of the involvement of ARID4B in senescence required the production of two antibodies, one for the isoform of ARID4B with the chromo domain (Epitope #2, Figure 3) and one for a region of ARID4B that is found in both isoforms and is not homologous to ARID4A (Epitope #1, Figure 3). The antibodies are being produced by immunization of rabbits with purified recombinant ARID4B domains.

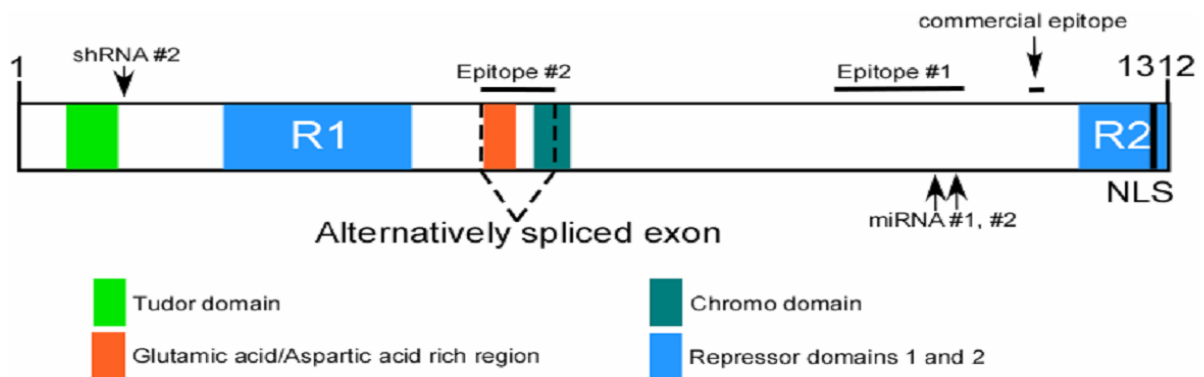


Figure 3: Primary structure of ARID4B. The alternatively spliced exon of ARID4b contains the glutamic acid/aspartic acid rich region and part of the chromo domain; this exon is predicted to be a second isoform of ARID4b. Epitopes 1 and 2 are labeled along with the commercially available antibody epitope.

Prohibitin

Prohibitin is a growth regulatory protein that has pleiotropic effects in the nucleus, mitochondria, and cytoplasm of the cell. Additionally, prohibitin plays a role in senescence but its exact role has yet to be identified. Prohibitin colocalizes with the heterochromatin protein, HP1 γ , and contributes to SAHF formation in DNA damage induced senescence in MCF-7 human breast cancer cells. In these cells, siRNA mediated knockdown of prohibitin results in significant reduction of HP1 γ recruitment to SAHF

and HP1 γ also dissociated from E2F promoters (Rastogi, 2006). Therefore, prohibitin appears to be important for cell cycle exit in cancer cells.

The role of prohibitin has yet to be studied in primary human cell lines. In order to study the role of prohibitin during the onset of senescence in human primary fibroblasts, cell lines with overexpressed prohibitin and with the depletion of prohibitin need to be produced. Through the use of lentiviruses and retroviruses, constitutive and inducible systems for the knockdown and overexpression of prohibitin will be used in our studies of senescence.

ASF1a (anti-silencing function 1 a)

ASF1a is a chromatin regulating protein that is required for formation of senescence associated heterochromatin foci (SAHF) and cell cycle arrest during senescence. ASF1a works in cooperation with another chromatin regulating protein, HIRA to drive formation of SAHF in WI38 human diploid fibroblasts (Zhang, 2005). The ASF1a/HIRA pathway works in parallel with the Rb pathway and cooperates with p53 and Rb to form SAHF (Ye, 2007).

Further investigation needs to be done to determine if ARID4B, prohibitin, ASF1a, and HIRA work in the same or different senescence pathways. Overexpression and RNAi experiments with all these proteins should be performed on human primary cell lines (WI38, IMR90, and BJ) and human transformed cell lines (U2OS, MCF-7, etc.). Before developing these cell lines, the ARID4B antibodies had to be produced and the best conditions to infect WI38 cells with lentiviruses had to be determined. This project focuses on the production of the ARID4B antibodies and the development of ASF1a and prohibitin knockdown cell lines.

Methods

Cell Culture

WI38 fibroblast cells were cultured in Dulbecco's Modified Eagle Medium (DMEM-GIBCO) supplemented with 10% fetal bovine serum (FBS), 1% L-glutamine, and 1% Antibiotics (GIBCO). Cells were grown in a 37°C, 5% CO₂ incubator. When the cells reached 75-100% confluency, cells were trypsinized, counted using a hemocytometer, and split into appropriate dishes. Population doublings were counted using standard procedures.

Immunofluorescence (IF)

Cells were grown on an 8 well IF slide. Media was removed, the cells were washed with Phosphate Buffered Saline (PBS, 10mM sodium phosphate, pH 7.4, 150 mM NaCl), and were fixed in 4% paraformaldehyde in PBS on ice. Cells were permeabilized with 0.5% Triton X-100 in PBS then blocked in 0.5% BSA/ 0.2% fish skin gelatin in PBS. The cells were then incubated in the ARID4B primary antibodies (1:500 dilution) and PML antibodies (Santa Cruz Biotechnologies, 1:800) for one hour at room temperature. FITC (1:400), Cy-5 (1:600) and Cy-3 (1:600) secondary antibodies were used to stain the cells. The DNA was visualized using DAPI (130 µg/mL). Slides were observed under a Zeiss Axioscope.

Immunoblots

Cells were resuspended in lysis buffer (20mM Tris-HCl pH 7.5, 1% SDS, 10% Glycerol) and the DNA was sheared using a 261/2 gauge needle. Cellular debris was removed by

centrifugation and protein concentration was determined using a Bradford assay with a BSA standard curve. Samples (with running buffer added) were run on appropriate percentage SDS- polyacrylamide gels under denaturing conditions at 150 V for about 2 hours. The samples were transferred by electroblotting to PVDF (polyvinylidene fluoride) membranes overnight at 100 mA. Membranes were blocked with 5% powder milk solution then probed with primary antibodies to ASF1a (1:300), ARID4B (1:1,000), or prohibitin (1:1,000) for 1 hour. Horseradish Peroxidase (HRP) coupled secondary antibodies (1:10,000) were used for the detection.

Transfection of 293T Cells to Generate Lentiviruses

Human embryonic kidney, 293T cells were plated at 6×10^6 cells per 10 cm dish. Plasmid DNA was grown in *E. coli* and isolated using a Qiagen plasmid midi prep kit. A packaging mix was made with 2.4 μg of VSV-g envelope glycoprotein, 10 μg of the transfer vector DNA, and 15 μg of Lp1 and 6 μg of Lp2 in 2.3 mL OPTI-MEM (Invitrogen). The packaging mix was combined with an equal volume of OPTI-MEM containing 2.4% Lipofectamine 2000 and the liposome/DNA complex was added to the dish for the transfection. The media was removed 12-18 hours post transfection and replaced with OPTI-PRO media. At the 48 and 72 hour time points, the supernatant was collected, pooled together, filtered through a 0.2 μm filter and stored at -80°C until needed to infect cells. Viral titers were then determined as described below.

Transfection of 293gag/pol Cells to Generate Retroviruses

Human embryonic kidney, 293gag/pol cells were grown in 10 cm. dishes at 6×10^6 cells per dish. Plasmid DNA was grown in *E. coli* and isolated using a Qiagen plasmid midi prep kit. A packaging mix was made with 2.4 μg of VSV-g envelope glycoprotein, 10 μg

of the transfer vector DNA, and 1.2 µg of plasmid gag/pol to form a viral complex. The transfection procedure, collection of viral supernatant and determination of viral titers was done in the same method as the lentiviruses (see above).

Viral Titers of Lentiviruses and Retroviruses

HT1080 cells were grown in 6 well plates at 25,000 cells per well. Lentivirus stocks were added to DMEM + Polybrene (Sigma, 6 µg/mL) in serial dilutions (total volume/well = 1 mL). Dilutions were added to the cells and plates were incubated at 37°C overnight. Media was replaced the next day and the appropriate selection antibiotics were added 2 days post infection. After incubation at 37 °C for 10-14 days, when colonies were visible, cells were fixed on ice with cold methanol. Cells were then stained with 0.5% crystal violet staining solution (25% methanol). Blue stained colonies were counted in each dilution to determine the titer of the retrovirus or lentivirus.

Infection of Primary and Transformed Human Cells with Lentiviruses and Retroviruses

WI38 primary fibroblasts and U2OS transformed cells were grown on 6 well plates at 100,000 cells per well. Cells were infected with 8,000 cfu (colony forming units) of virus, as determined by viral titers, mixed with DMEM + polybrene (6 µg/mL) and incubated for overnight at 37°C. Selection antibiotics were added 2 days after infection.

Protein Purification of the ARID4B domain and ARID4B exon 16

The ARID4B domains were fused to GST at the N-terminus for purification using the pGEX GP-1 plasmid (Amersham). The ARID4B GST fused protein plasmids were mixed with competent *E. coli* Rosetta cells and incubated for 20 minutes at room temperature. The mixture was then heat shocked (42°C) for 30 seconds. The cells were agitated in SOC broth at 37°C for one hour. A pre-warmed agar plate was used to plate the cells and

incubated overnight at 37°C. One colony was picked from each plate and inoculated overnight at 37°C in 4 mL LB broth. A 50 mL culture was grown overnight then diluted 1:500 in 1L flasks (3 L for ARID4B domain; 9 L for ARID4B exon 16) of YT (yeast-triptone) media. When the culture reached log phase ($A_{600} = 0.5$) Isopropyl β -D-1-thiogalactopyranoside (IPTG) was used to induce the cultures, which were then grown overnight at room temperature. The cultures were centrifuged at 7000 rpm for 7 minutes. The pellet was resuspended in 60 mL of PBS containing protease inhibitors (aprotinin, benzamide, leupeptin, phenylmethylsulphonyl fluoride (PMSF), E64, pepstatin, and phosphoramidon) and sonicated. The cellular debris was removed by ultracentrifugation at 40,000 rpm for 45 minutes in a 45Ti ultracentrifuge rotor then filtered through a 0.45 μ m filter.

Glutathione Sepharose Column Purification

The *E. coli* cell lysate was incubated with glutathione Sepharose (binds GST) beads for 2 hours at 4°C. The lysate and glutathione sepharose resin was then poured in a column and the flow through was collected. The column was then washed 3 times with 50 mL of PBS containing 350 mM NaCl. The ARID4B domain-GST fusion protein was eluted from the column with elution buffer (50 mM Tris-HCl pH 8.0, 10 mM Glutathione, 1 mM DTT) and dialyzed overnight in PreScission cleavage buffer (50 mM Tris-HCl pH 7.5, 150 mM NaCl, 1 mM EDTA, 1 mM DTT). PreScission protease fused to GST (Amersham Biosciences) was added to the dialysis bag at 0.16 mg/mL of resin and incubated for 4 hours. The solution was then put back on the column and collected (eluate) to run on an SDS-PAGE gel. The ARID4B exon 16-GST fusion protein was incubated with the

PreScission cleavage buffer and GST fused protease overnight then eluted from the column and collected (eluate) to run on an SDS-PAGE gel.

Q Sepharose Column Purification

The ARID4B domain and ARID4B exon 16 were further purified on a Q sepharose column using an AKTA Explorer (Pharmacia). The column was equilibrated with low salt buffer A (150mM NaCl, Tris-HCl pH 7.5). The sample was loaded on the column and eluted with a salt gradient from low salt (150mM NaCl) to high salt (1 M NaCl).

Peak fractions were selected by absorbance at 280 nm.

CuCl₂ Staining, Electroelution, and Lyophilization

The exon 16 sample was concentrated in a CentriPrep tube (1000 Da MW cutoff) and loaded (1.6 mL) on a 40 mL 20% SDS-PAGE gel. After electrophoresis, the gel was washed with distilled water, several changes over 30 seconds. The gel was negatively stained with 200 mL of 0.3M CuCl₂ and incubated with agitation for 5 minutes at room temperature. The largest clear band (MW ~10 kDa) was cut from the gel and placed in a dialysis bag (3,000 Da MW cutoff) containing 1 mL (0.2M Tris/Acetate pH 7.4, 1% SDS, 100mM DTT)/0.1 g wet polyacrylamide gel for electroelution. The dialysis bag and running buffer (50mM Tris/Acetate pH 7.4, 0.1% SDS, 0.5mM sodium thioglycolate) were placed in an electrophoresis chamber and ran at 100 V (about 100 mA) for 3 hours. The solution was then dialyzed in 0.2M sodium carbonate and 0.02% SDS with several changes over 4 hours at 4°C. The protein solution was removed and lyophilized overnight. The protein was resuspended in 10 mL of distilled water and lyophilized a second time, then resuspended in 4 mL distilled water.

Results

ARID4B Domain and Exon 16 Antibody Purification and Production

Before investigating the role of ARID4B in senescence, antibodies for the two isoforms of ARID4B were needed because the one commercially available antibody did not detect overexpressed ARID4B on an immunoblot. Two domains of the ARID4B protein were chosen to be purified; the first was a domain (17 kDa) found in both isoforms of ARID4B that is not homologous to ARID4A (Epitope #1, Figure 3). The second region was the alternatively spliced exon (exon 16, 10 kDa) that contains the chromo domain (Epitope #2, Figure 3).

Both the epitope 1 ARID4B domain and the ARID4B exon 16 proteins were fused to Glutathione S- Transferase (GST) at the N-terminus then overproduced in *E.Coli*. Purification began with a glutathione sepharose column. The epitope 1 ARID4B domain was eluted from the column, and then dialyzed and cleaved with protease (Figure 4), while exon 16 was eluted and cleaved with protease from the column with no dialysis (Figure 5). The domain of ARID4B had a predicted molecular weight of 17 kDa but it actually migrated at about 35 kDa (Figure 4), coinciding with the previous report that ARID4B migrates at a higher molecular weight on SDS-PAGE gels than expected (Fleischer, 2003). Exon 16 ran at the expected 10 kDa (Figure 5).

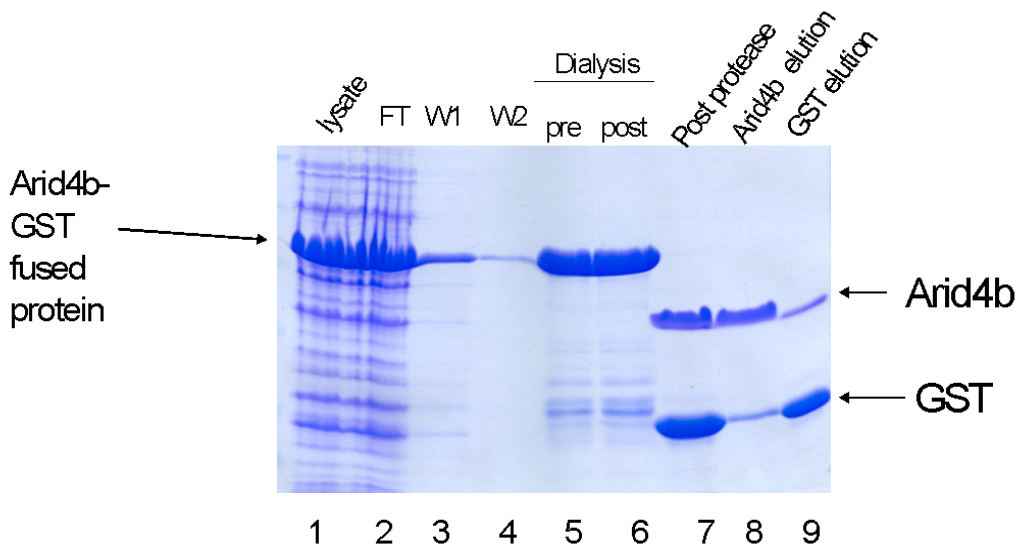


Figure 4: Glutathione Sepharose column purification of the epitope 1 ARID4b domain. The cell lysate was poured over the column the flowthrough (FT, lane 2) was collected. The column was then washed with chilled phosphate buffered saline (PBS) (W1 and W2, lanes 3 and 4). The GST-ARID4b fusion protein was then eluted off the column (lane 5), dialyzed (lane 6), then cleaved with protease. Lane 7 is the contents of the dialysis bag post protease (still contains GST, MW 26 kDa, and the epitope 1 ARID4B domain, MW 35 kDa) and lane 8 is the elution of the epitope 1 ARID4B domain post GST cleavage from the glutathione sepharose column. Lane 9 is the elution of the leftover bound GST on the column.

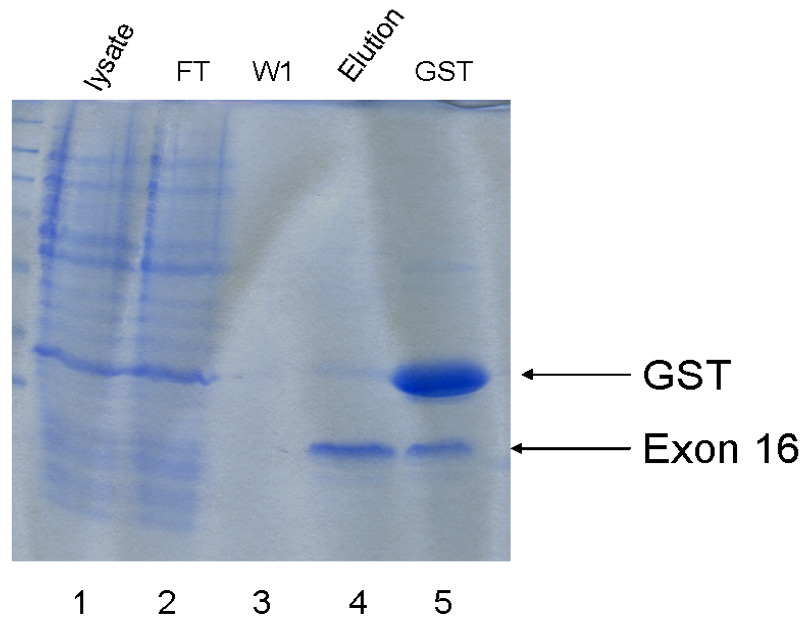


Figure 5: Glutathione Sepharose column purification of ARID4b exon 16. The cell lysate was poured over the column and the flowthrough (FT, lane 2) was collected. After the washing of the column (W1, lane 3), the ARID4B exon 16 protein was cleaved off the column. Lane 4 shows the elution of Exon 16 (MW, 10 kDa) post protease. GST elution (MW, 26 kDa) from the column post protease is shown in lane 5.

The epitope 1 ARID4B domain and ARID4B exon16 proteins had to be highly purified before the antibodies could be produced to reduce cross reactivity with other proteins. The epitope 1 ARID4B domain and exon 16 purifications were both determined to contain excess GST post elution from the column, therefore requiring further purification. Both proteins were found to have a negative charge at pH 7 so a Q sepharose column was used as the next step in the purification process (Figures 6 and 7).

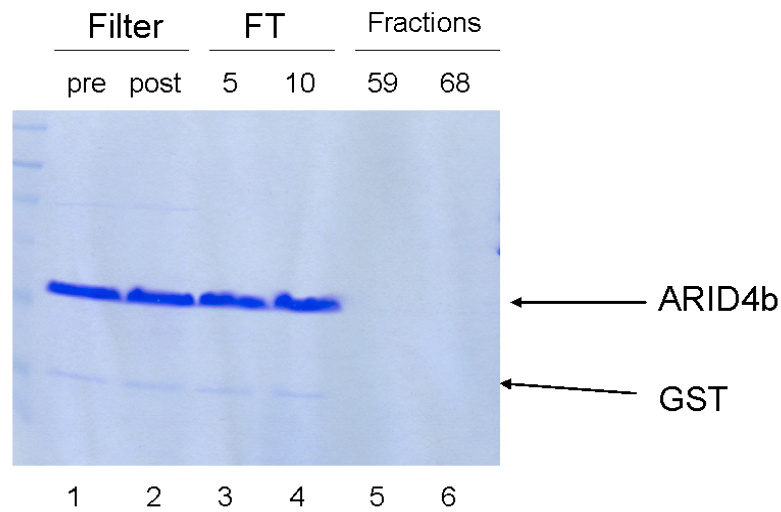


Figure 6: Q sepharose column purification of the epitope 1 ARID4B domain. The epitope 1 ARID4B domain eluted in the flow through (FT, lanes 3 and 4, MW 35 kDa) of the Q sepharose column instead of in the fractions (lanes 5 and 6) where it was predicted to elute. Lanes 1 and 2 show the sample before and after being filtered prior to injection in the AKTA.

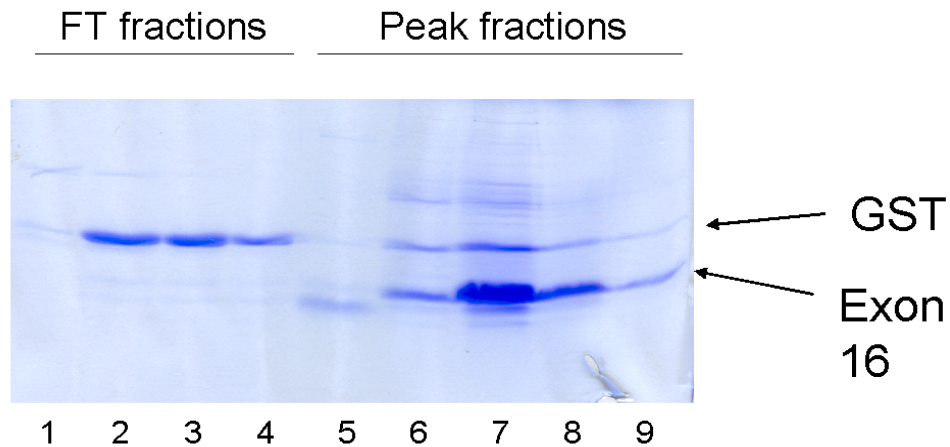


Figure 7: Q sepharose column purification of ARID4b exon 16. The exon 16 protein eluted in the peak fractions (lanes 5-9, MW 10 kDa) from the Q sepharose column as predicted. The Flow through (FT, lanes 1-4) contained GST (MW 26 kDa) and other faint unknown protein bands.

The Q sepharose column purification of the epitope 1 ARID4B domain left very little GST in the solution (Figure 6). Enough protein was generated to be sent to the Pocono Rabbit Farm and Laboratory Inc. to begin production of the ARID4B antibody. The first bleed of the antibody production was received and tested on an immunoblot (Figure 8). The molecular weight of ARID4B is about 150 kDa but the protein was detected on the western blot at 200 kDa, as previously reported (Fleischer, 2003). These results show that the ARID4B can be detected endogenously and by overexpression on an immunoblot.

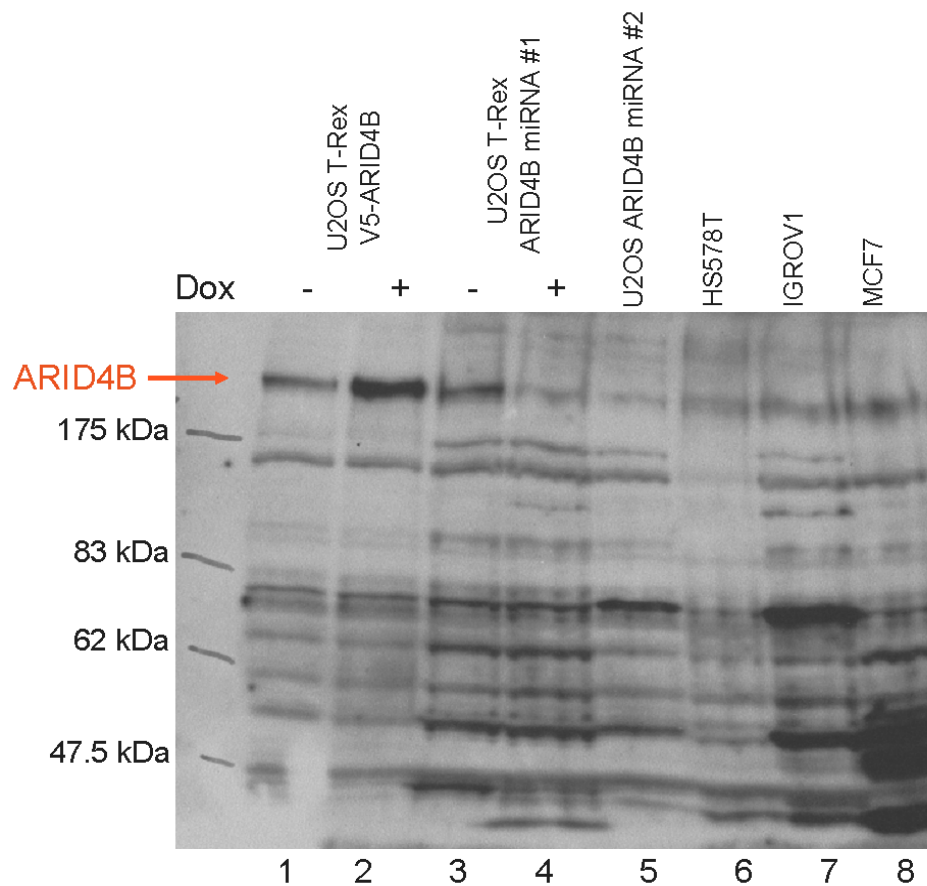


Figure 8: Immunoblot of the first bleed of the ARID4b antibody. The antibody recognizes a 200 kDa protein, predicted to be ARID4B. The V5 tagged ARID4B overexpression induced by doxycycline in U2OS cells is detected by the antibody (lanes 1 and 2). The miRNA silencing of ARID4b induced by doxycycline in U2OS cells is also detected by the antibody (lanes 3 and 4). The silencing of ARID4B by a second, constitutive miRNA expressed in U2OS cells was also detected (lane 5). IGROV1, an ovarian cancer cell line, and MCF7, a breast cancer cell line, are shown to express truncated versions of ARID4B at MW 50 and 40 kDa in MCF-7 and, 80 and 52 kDa in IGROV-1 (lanes 7 and 8). (Data from Eric Campeau, PhD)

The epitope 1 ARID4B domain antibody was also tested by immunofluorescence (IF). ARID4B foci were detected with the antibody and were observed to colocalize with PML bodies in WI38 cells at 96 hours post x-ray irradiation (10 Gy) (Figure 9). ARID4B foci did not colocalize with SAHF at this time point (Figure 9). Further experimentation needs to be done to confirm these results. This IF assay was done primarily to prove the antibody can detect ARID4B through immunofluorescence. These results, along with the immunoblot results indicate that the antibody produced for the epitope 1 ARID4B domain was sufficient to detect the presence of ARID4B in both assays.

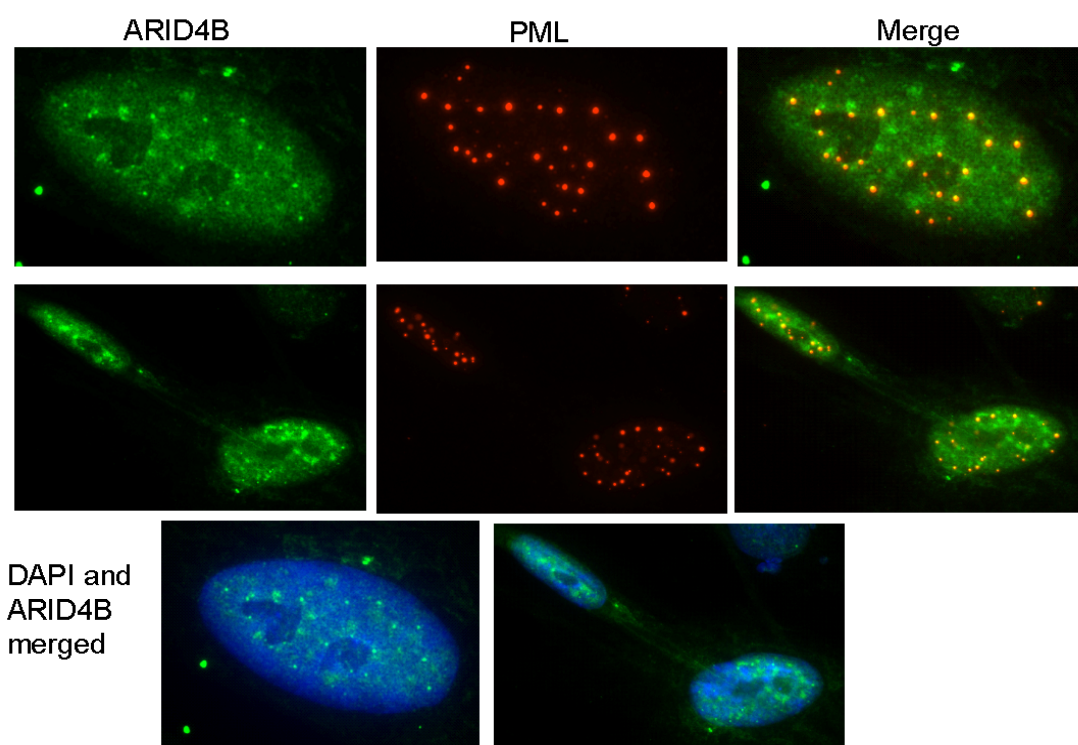


Figure 9: Immunofluorescence detection of ARID4B. WI38 primary human fibroblasts were infected with lentiviral ARID4B. The cells were irradiated on the IF slide and the slide was observed 96 hours post irradiation. DAPI was used to detect SAHF. (Data from Eric Campeau, PhD)

In the purification of ARID4B exon 16 from the Q sepharose column (Figure 7), other bands were still stained in the gel, presenting the need for further purification. The

protein was run in a large 20% SDS-PAGE gel (Figure 10). The gel was negatively stained with CuCl_2 and the ARID4B exon 16 band was cut from the gel. Electroelution was done to remove the protein from the gel. After lyophilization of the protein, it was determined by running the sample on a SDS-PAGE gel that there was not enough protein to start production of the antibody (Figure 11). Another 9 L of exon 16-GST culture was grown and purified in the same process as described above. The ARID4B exon 16 antibody is now in production at the Pocono Rabbit Farm and Laboratory Inc, 2 bleeds have been received but have been unsuccessful in detecting ARID4B on an immunoblot. (Second purification completed by Eric Campeau, PhD)

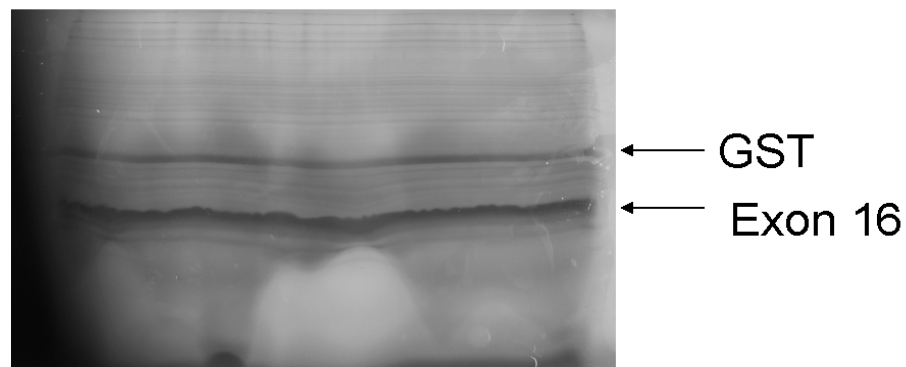


Figure 10: Copper chloride (CuCl) negatively stained gel of ARID4B Exon 16. The ARID4B exon 16 band (MW 10 kDa) was cut out of the gel, electroeluted, and then lyophilized.

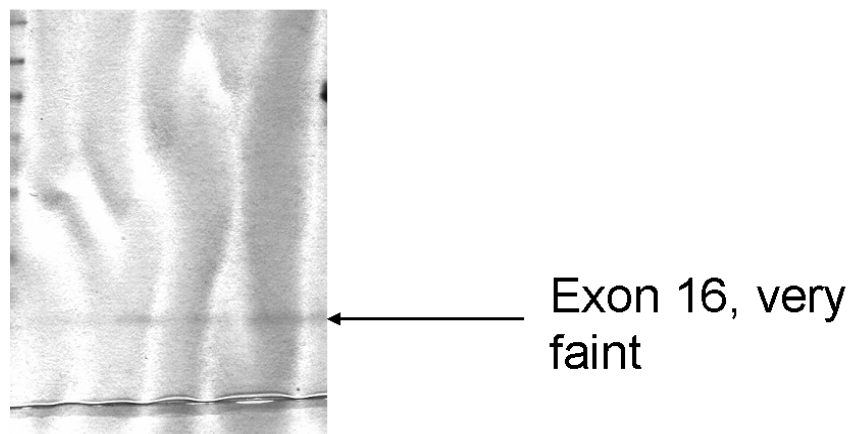


Figure 11: ARID4B exon 16 post lyophilization. The only band present in the final purification was the ARID4B exon 16 band (MW 10 kDa).

In summary, we were able to overexpress and purify two domains of ARID4B in order to generate rabbit polyclonal antibodies that can be used to study both isoforms of the ARID4B protein and their possible role in establishing or maintaining senescence.

Depletion of Prohibitin with Retroviral miRNA

Constitutive miRNA retroviruses against prohibitin were produced to perform senescence studies with human cell lines with depleted prohibitin. After infection of U2OS cells, a human osteosarcoma cell line, and HT1080 cells several times, it was shown that cells do not survive the constitutive miRNA mediated depletion of prohibitin (Figure 12). A small amount of cells infected with miRNA against prohibitin survived after selection. However, more of the control GFP (green fluorescence protein) infected cells survived the selection. At day 1, in the area observed in the GFP infection 3 cells were present, which grew to 4 cells by day 4. On day 8 there were 5 cells present but the cells moved around the well not allowing all 5 cells to be in the field of view when the picture was taken (Figure 12, top row). Three cells were also present in the area observed for the miRNA prohibitin infection. On day 4, 2 of the cells look to be fused together and by day 8 only one cell was left (Figure 12, bottom row). The pictures were representative of most of the well in each infection however, a few cells did grow in the miRNA against prohibitin infection, but these cells probably represent the few that did not have depletion of prohibitin. This is known because in a previous experiment cells were left to grow for 2-3 weeks but when tested, did not show depletion of prohibitin by immunoblot (data not shown). These results show that experiments with constitutive depletion of prohibitin by might not be possible.

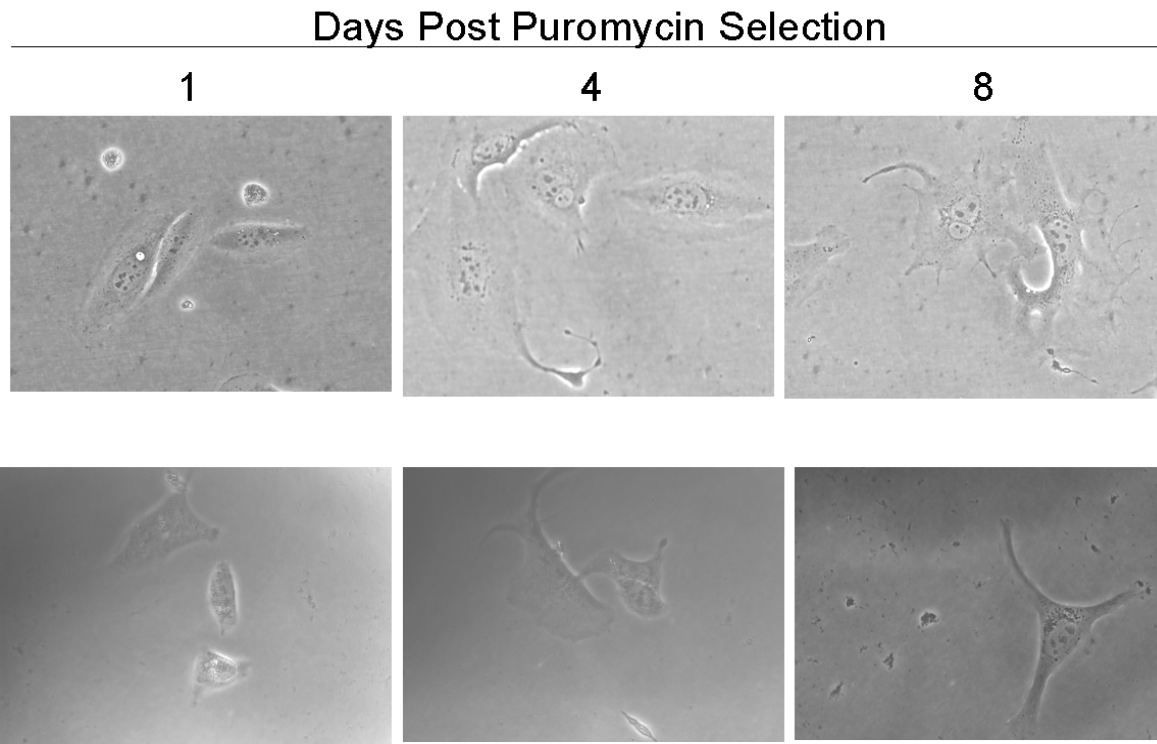


Figure 12: Depletion of prohibitin Results in Cell Death in U2OS cells. U2OS cells were infected with retroviruses encoding GFP (green fluorescent protein, top row) or miRNA against prohibitin (bottom row) Infected cells were selected for puromycin resistance and were observed over on a daily basis for 8 days post selection to monitor growth with puromycin. As shown on the top row, cells infected with GFP proliferate whereas cells with depleted prohibitin stop growing and eventually die.

Depletion of ASF1a with Lentiviral miRNA

In order to see the effects of senescence in cells with depleted ASF1a, a working miRNA directed against ASF1a was needed. Constitutive lentiviral miRNAs directed against ASF1a were produced in 293T cells and tested to determine how efficiently each miRNA depleted ASF1a. The constitutive lentiviral system was compared with an inducible system already known to effectively deplete ASF1a (Figure 13). Both miRNA #1 and #2 depleted close to 90% of the endogenous level of ASF1a (Figure 13). These results indicate that we will be able to use the constitutive lentiviral system to study the effect of ASF1a depletion in senescence.

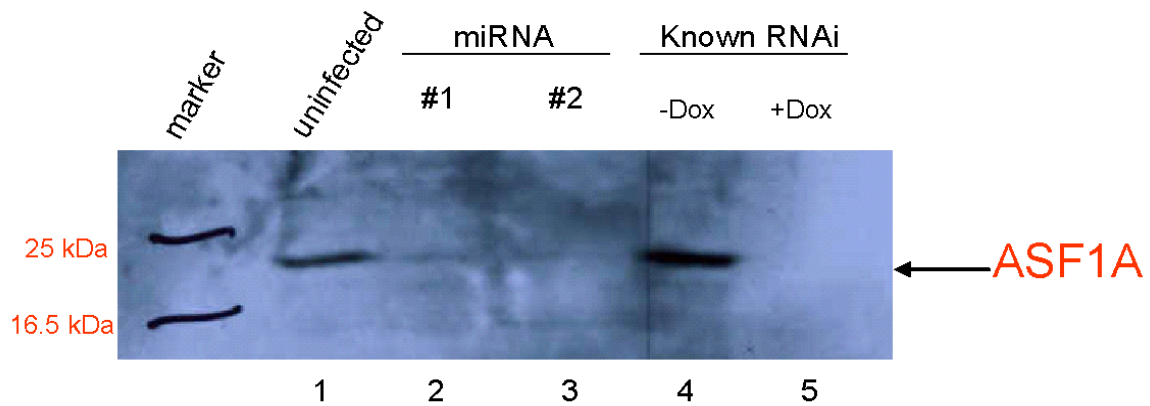


Figure 13: miRNA Depletion of Asf1a in U2OS cells. Endogenous ASF1a was detected in the uninfected U2OS cells (lane 1) but not in the cells expressing miRNAs #1 and #2 (lanes 2 and 3). A known, doxycyclin inducible RNAi for ASF1a was used as a positive control (lanes 4 and 5).

Discussion

ARID4B

The two chosen epitopes of ARID4B, the domain not homologous to ARID4A and exon 16 with the chromo domain, were overexpressed in *E. coli* and purified to produce ARID4B antibodies. The production of the epitope 1 ARID4B domain is currently coming to an end. The fifth bleed of the rabbit polyclonal antibody has been received and is now being purified to make the antibody more specific to ARID4B.

The epitope 1 ARID4B domain antibody has been tested in an immunoblot (Figure 8), immunofluorescence (Figure 9), and immunoprecipitation (data not shown). ARID4B was successfully detected in all three assays. This will provide a valuable tool for the characterization of truncations of the ARID4B protein in breast cancer cells as well as identifying the cellular localization and composition of ARID4B complexes in proliferating and senescent cells.

The second epitope of ARID4B, exon 16—with the chromo domain is currently in the process of being produced at Pocono Rabbit Farm and Laboratory Inc. At this time, two bleeds have been received but the serum from both bleeds was not successful in detecting ARID4B on an immunoblot. The third bleed will be tested when it is received and if ARID4B is still not detected, another peptide will be synthesized from exon 16 that does not contain the glutamic acid/aspartic acid repeats or the chromo domain. If the third bleed is successful in detecting ARID4B, identification of both isoforms of ARID4B in human breast cancer cells and primary fibroblasts will be possible.

Prohibitin

U2OS human osteosarcoma cells did not survive the constitutive retroviral miRNA mediated depletion of prohibitin. Several attempts to deplete prohibitin in U2OS cells (Figure 12) and HT1080 cells (data not shown) resulted in cell death. This result needs to be confirmed by generating a doxycycline inducible system of depleting prohibitin, which is currently in the process of production in the laboratory. Other cell lines with inducible knockdown systems have been successfully made, such as ASF1a (Figure 13) and ARID4B (Figure 8). With the inducible system the cells do not need to be continually infected and the level of induction mediated by the concentration of doxycycline can alter the amount of protein depleted in the cells, relieving the amount of the stress on the cells. Generating the inducible system for the depletion of prohibitin will identify if cells can survive with the knockdown of prohibitin and if the constitutive system killed the cells from the combined stresses of infection and depletion of prohibitin in the cells.

Generating a cell line with the depletion of prohibitin will allow investigation of the role of prohibitin in cellular senescence. In MCF-7 human breast cancer cells, the knockdown of prohibitin was shown to inhibit recruitment of HP1 γ to SAHF and cause dissociation of HP1 γ from E2F promoters (Nastogi, 2006). This could cause the bypass of senescence in human primary fibroblasts, and can be further studied when production of a working knockdown of prohibitin in human primary fibroblasts is complete.

ASF1a

Production of a constitutive lentiviral miRNA mediated depletion of ASF1a was successful. One study has shown that ASF1a is required for the onset of senescence (Zhang, 2005), but the role of ASF1a in the maintenance of senescence has yet to be studied. The successful knockdown of ASF1a will allow for the study of the role of ASF1a in the maintenance of cellular senescence and further investigation of ASF1a's role in the onset of senescence. Lentiviruses are able to replicate in senescent, non-proliferating cells, while the expression of retroviruses requires that the cells be dividing. The lentiviral miRNA can also be used to knockdown ASF1a in cells that have already become senescent to study if ASF1a is required for the maintenance of the senescent phenotype.

Conclusions

The work done in this project for all three proteins, ARID4B, prohibitin, and ASF1a can be used in conjunction to identify how all three proteins work together in cellular senescence. Experiments can be done with depleted ASF1a cell lines and overexpression of ARID4B or prohibitin, and all other combinations of the three proteins.

These experiments will show how the onset of senescence is affected by different combinations of knockdown and overexpression.

Determining the function of ASF1a, ARID4B and prohibitin in the onset and maintenance of cellular senescence could eventually prove to be essential in inducing senescence in human malignant tumors. Cancer therapeutic agents designed to induce senescence in human cancers are of high interest at this time. The knowledge of the three proteins in this project could one day aid in the development of new cancer therapeutic agents or agents that would maintain the state of senescence in premalignant tumor cells.

References

- Beauséjour, C., Krtolica, A., Galimi, F., Narita, M., Lowe, S., Yaswen, P., Campisi, J. (2003) *EMBO* **22**, 4212-4222.
- Ben-Porath, I., Weinberg, R. (2005) *Int. J. Biochem. Cell Biol.* **37**, 961-976.
- Braig, M., Soyoung, L., Loddenkemper, C., Rudolph, C., Peters, A., Schlegelberger, B., Stein, H., Dorken, B., Jenuwein, T., Schmitt, C. (2005) *Nature* **436**, 660-665.
- Campisi, J., Kim, S., Lim, C., Rubio, M. (2001) *Exp. Gerontol.* **36**, 1619-1637.
- Campisi, J. (2005) *Cell* **120**, 513-522.
- Campisi, J. (2005) *Science* **309**, 886-887.
- Cao, J., Gao, T., Stanbridge, E., Irie, R. (2001) *J. Natl. Cancer Inst.* **93**, 1159-1165.
- Chen, Z., Trotman, L., Shaffer, D., Lin, H., Dotan, Z., Niki, M., Koutcher, J., Scher, H., Ludwig, T., Gerald, W., Cordon-Cardo, C., Pandolfi, P. (2005) *Nature* **436**, 725-730.
- Cui, D., Jin, G., Gao, T., Sun, T., Tian, F., Estrada, G., Gao, H., Sarai, A. (2004) *Cancer Epidemiol. Biomarkers Prev.* **13**, 1136-1145.
- Dimri, G., Lee, X., Basile, G., Acosta, M., Scott, G., Roskelley, C., Medrano, E., Linksens, M., Rubelj, I., Pereira-Smith, O., Peacocke, M., Campisi, J. (1995) *Proc. Natl. Acad. Sci.* **92**, 9363-9367.
- Dimri, G. (2005) *Cancer Cell* **7**, 505-512.
- Fleischer, T., Yun, U., Ayer, D. (2003) *Mol. Cell Biol.* **23**, 3456-3467.
- Narita, Masashi, Nunez, S., Heard, E., Narita, Masako, Lin, A., Hearn, S., Spector, D., Hannon, G., Lowe, S. (2003) *Cell* **113**, 703-716.
- Rastogi, S., Joshi, B., Dasgupta, P., Morris, M., Wright, K., Chellappan, S. (2006) *Mol. Cell Biol.* **26**, 4161-4171.
- Serrano, M., Lin, A., McCurrach, M., Beach, D., Lowe, S. (1997) *Cell* **88**, 593-602.
- Ye, X., Zerlanko, B., Zhang, R., Somaiah, N., Lipinski, M., Salomoni, P., Adams, P. (2007) *Mol. Cell Biol.* Published Online Ahead of Print.
- Zhang, R., Poustovoitov, M., Ye, X., Santos, H., Chen, W., Daganzo, S., Erzberger, J., Serebriiskii, I., Canutescu, A., Dunbrack, R., Pehrson, J., Berger, J., Kaufman, P., Adams, P. (2005) *Dev. Cell* **8**, 1-20.

